

SUPPORTING INFORMATION

Electrodynamics of soft multilayered particles dispersions: Dielectric permittivity and dynamic mobility.

Jenny Merlin,^{1,2*} Jérôme F.L. Duval^{1,2}

¹ Université de Lorraine, Laboratoire Interdisciplinaire des Environnements Continentaux (LIEC),
UMR 7360, 15 avenue du Charmois, Vandœuvre-lès-Nancy, F-54501, France.

² CNRS, Laboratoire Interdisciplinaire des Environnements Continentaux (LIEC), UMR 7360, 15
avenue du Charmois, Vandœuvre-lès-Nancy, F-54501, France.

*Corresponding author. Email: merlin@sdu.dk

jennymerlin@hotmail.fr

Current address: Institute for Physics, Chemistry and Pharmacy, University of Southern Denmark,
Campusvej 55, 5230 Odense, Denmark.

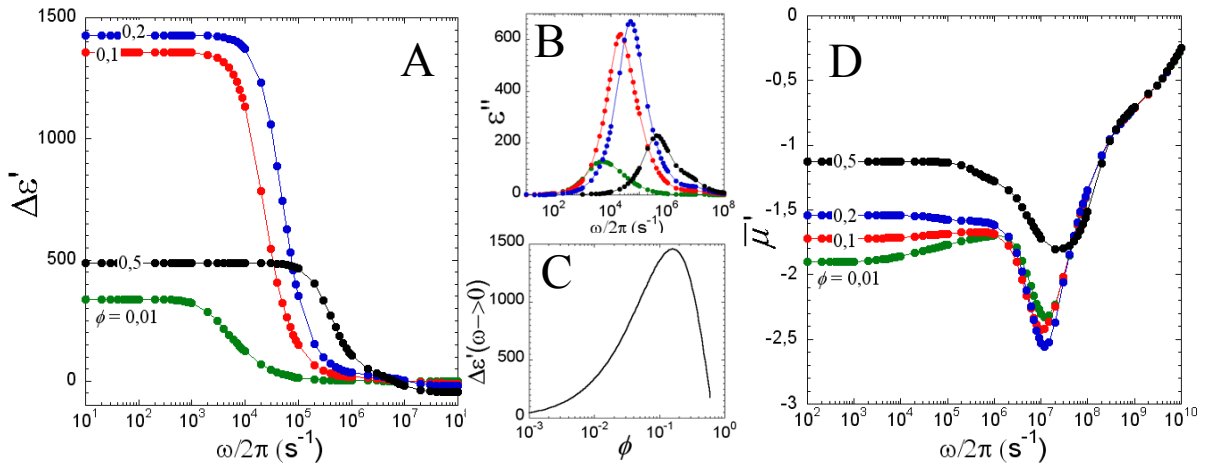
Impact of the particle volume fraction on the dielectric permittivity and dynamic mobility

The dependence of the dielectric increment $\Delta\varepsilon'(\omega)$ on frequency $\omega/2\pi$ is displayed in Figure S1A for various values of particle volume fractions ϕ while keeping the hard core radius a constant. The variation of ϕ is performed under the condition $a + d_1 + d_2 + \kappa^{-1} < b$ in order to avoid the overlapping of polymeric segments and electric double layers of two neighboring particles. All the other parameters are fixed and are reported in the caption of Figure S1. Figure S1B represents the corresponding variations of the dielectric loss $\varepsilon''(\omega)$. Let us first consider the low frequency regime, *i.e.* $\omega/2\pi < 10^3 \text{ s}^{-1}$. $\Delta\varepsilon'(\omega)$ increases with increasing ϕ from 0.01 to 0.2 and then decreases upon further increase of ϕ from 0.2 to 0.5. In order to understand the mechanism responsible for this apparent non-monotonous variation of $\Delta\varepsilon'(\omega)$ with ϕ , we report in Figure S1C the quantity $\Delta\varepsilon'(\omega \rightarrow 0)$ as a function of ϕ . For very diluted dispersions of particles ($\phi \ll 1$), a permittivity closed to 0 is obtained, as expected. In this situation, the dispersion contains a large amount of medium compared to that of solids. As a result, the α -relaxation process taking place around the few particles in the solution does not significantly impacts the overall dielectric response of the suspension. $\Delta\varepsilon'(\omega \rightarrow 0)$ then increases with increasing ϕ up to a critical value ($\phi = 0.2$) and drastically drops upon further increase of ϕ . The initial increase in the magnitude of $\Delta\varepsilon'(\omega \rightarrow 0)$ is simply due to the increasing amount of fixed charges in the dispersion. The drop in the magnitude of

35 $\Delta\varepsilon'(\omega \rightarrow 0)$ observed for large ϕ has been discussed in detail in previous work.^{1, 2} As explained in
 36 the main text, the α -relaxation results from the establishment of an accumulation of neutral electrolyte
 37 on one side of the particle and a depletion of neutral electrolyte on the other side. For sufficiently large
 38 ϕ (in our case $\phi > 0.2$), the α -relaxation is reduced by the overlap of polarization regions of adjacent
 39 particles. Now consider frequencies $\omega/2\pi > \omega_{\text{MW}}/2\pi \approx 3 \cdot 10^7 \text{ s}^{-1}$. $\Delta\varepsilon'(\omega)$ decreases upon increase of ϕ .
 40 At such high frequencies, ions do not have time to migrate/diffuse in response to the applied electric
 41 field. The polarization is then mainly governed by the mismatch between permittivity of the dispersing
 42 medium ($\varepsilon_r = 78.4$) and that of the hard core of the particle ($\varepsilon_p = 2$). Because ε_p is much smaller than
 43 ε_r , the dielectric permittivity decreases with increasing ϕ .

44 From Figure S1A and B, it is shown that ω_α increases upon increase of ϕ . Let us comment on this.
 45 In the situation of diluted dispersions, the establishment of a concentration gradient leads to the
 46 diffusion of counterions from one side of the particle to the other with a the characteristic diffusion
 47 length. With increasing ϕ , the distance between two neighboring particles is reduced and becomes
 48 lower than a . The counterions then diffuse from one particle to the other and the characteristic
 49 diffusion length of that process decreases with increasing ϕ . The smaller this characteristic length, the
 50 larger is ω_α .

51



52

53 **Figure S1.** Variations of dielectric increment $\Delta\varepsilon'$ (panel A) and dielectric loss ε'' (panel B) as a function of
 54 field frequency $\omega/2\pi$ for various particle volume fractions ϕ (indicated). (Panel C) Variations of the magnitude
 55 of $\Delta\varepsilon'(\omega \rightarrow 0)$ as a function of ϕ . (Panel D) Variations of dimensionless dynamic mobility $\bar{\mu}$ as a function of
 56 $\omega/2\pi$ for various ϕ (indicated). Other parameters if not indicated in Table 1 (main text): $c^* = 1\text{mM}$; $\lambda_2^0 d_2 = 1$;
 57 $\beta_1 = \beta_1^H = 5$; $\rho_2^0 / F = -10\text{mM}$; $d_1 = 20\text{nm}$; $d_2 = 5\text{nm}$; $a = 300\text{nm}$; $\alpha_1 = \alpha_2 \rightarrow 0$; $z = 1$.

58

59 Note that ω_{MWO} does not depend on ϕ . Indeed, the Debye length κ^{-1} , *i.e.* the characteristic length
60 scale defining the MWO relaxation frequency, remains constant upon increase of ϕ (we excluded the
61 overlapping of the electric double layers of neighboring particles).

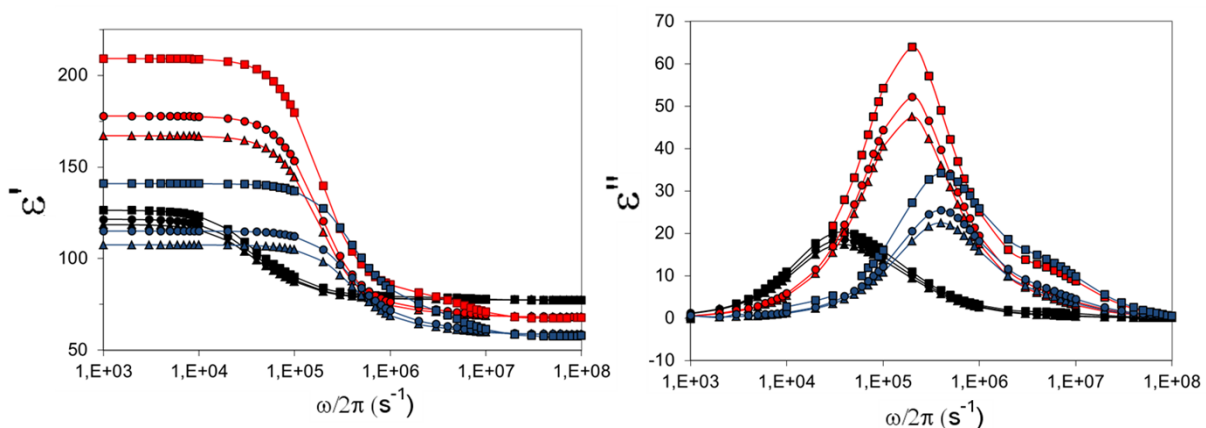
62 The counterparts of Figure S1A for the dynamic mobility are given in Figure S1D. Figure S1D
63 shows a decrease in magnitude of $\bar{\mu}'(\omega)$ and a slight increase in the characteristic frequency of
64 inertial relaxation with increasing ϕ . This negative contribution results from increasing particle –
65 particle hydrodynamic interactions that tend to hinder the motion of the particles.

66

67 *Verification of the outcome of the numerical code presented in this work*

68 In the limiting case where there is only one homogeneous polymeric layer surrounding the
69 particle core surface, we tested our numerical results with those obtained by Ahualli *et al.*¹ For the
70 sake of illustration, Figure S2 displays the dependence of the dielectric permittivity ε' and dielectric
71 loss ε'' on frequency $\omega/2\pi$ as obtained from our numerical procedure under the conditions adopted in
72 Figure 11 in reference [1]. Our results quantitatively agree with those obtained by Ahualli *et al.*

73



74

75 **Figure S2.** Variations of dielectric permittivity ε' and dielectric loss ε'' as a function of field frequency $\omega / 2\pi$
76 for various particle volume fractions $\phi = 0.01$ (black), $\phi = 0.1$ (red), $\phi = 0.2$ (blue) and various friction
77 parameters $\lambda_1^0 a = 1$ (squares), $\lambda_1^0 a = 10$ (circles) and $\lambda_1^0 a = 1$ (triangles). The particles consist of a hard core
78 covered by a unique homogeneous polymeric layer. Other parameters: $c^* = 1\text{mM}$; $d_1 = 50\text{nm}$; $a = 100\text{nm}$;
79 $\alpha_1 \rightarrow 0$; $z = 1$, total charge of the hard core = $1.67 \cdot 10^{-15}\text{C}$; total charge of the polymer layer = $1.4 \cdot 10^{-15}\text{C}$; $\varepsilon_p =$
80 4.5 , density $\rho_p = 2200 \text{ kg m}^{-3}$.

81

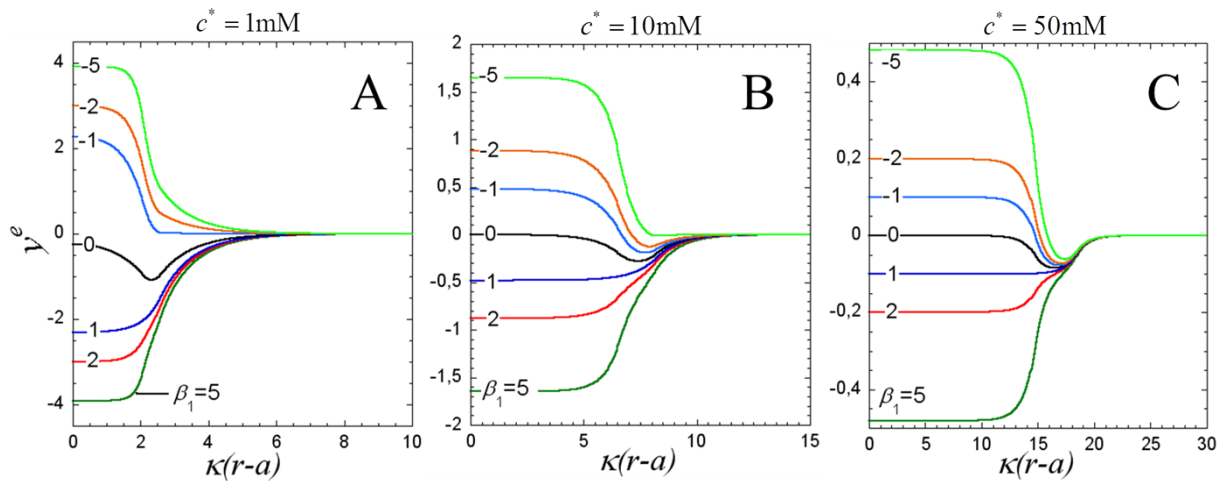
82

83

84

85

86

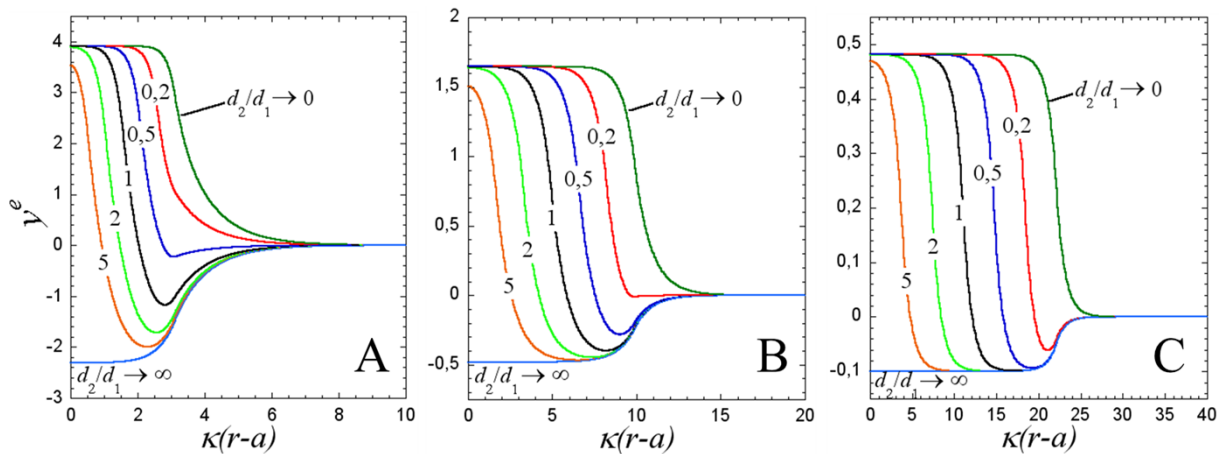


89

90 **Figure S3.** Dimensionless potential distribution from the core surface of the particle to the bulk
 91 solution under conditions of Figure 2 (main text) with various β_1 (indicated) and $c^* = 1\text{ mM}$ (panel
 92 A), $c^* = 10\text{ mM}$ (panel B) and $c^* = 20\text{ mM}$ (panel C). The outer layer is marked by the bump
 93 observed in the situation $\beta_1 = 0$.

94

95



96

97 **Figure S4.** Dimensionless potential distribution from the core surface of the particle to the bulk
 98 solution under conditions of Figure 5 (main text) with various d_2/d_1 (indicated) and $c^* = 1\text{ mM}$
 99 (panel A), $c^* = 10\text{ mM}$ (panel B) and $c^* = 20\text{ mM}$ (panel C).

100

101 **References**

102

- 103 1. S. Ahualli, M. L. Jiménez, F. Carrique and A. V. Delgado, *Langmuir*, 2009, 25, 1986-1997.
 104 2. F. Carrique, *Journal of Chemical Physics*, 2003, 118, 1945-1956.

105